Research Article

Cancer Immunology Research

# The Mutation-Associated Neoantigen Functional Expansion of Specific T Cells (MANAFEST) Assay: A Sensitive Platform for Monitoring Antitumor Immunity

Ludmila Danilova[1,2,3], Valsamo Anagnostou[1,2], Justina X. Caushi[1,2], John-William Sidhom[1,2], Haidan Guo[1,2], Hok Yee Chan[1,2], Prerna Suri[1,2], Ada Tam[1,2], Jiajia Zhang[1,2], Margueritta El Asmar[1,2], Kristen A. Marrone[1,2], Jarushka Naidoo[1,2], Julie R. Brahmer[1,2], Patrick M. Forde[1,2], Alexander S. Baras[1,2,4], Leslie Cope[1,2], Victor E. Velculescu[1,2], Drew M. Pardoll[1,2], Franck Housseau[1,2], and Kellie N. Smith[1,2]

## Abstract

Mutation-associated neoantigens (MANA) are a target of antitumor T-cell immunity. Sensitive, simple, and standardized assays are needed to assess the repertoire of functional MANA-specific T cells in oncology. Assays analyzing *in vitro* cytokine production such as ELISpot and intracellular cytokine staining have been useful but have limited sensitivity in assessing tumor-specific T-cell responses and do not analyze antigen-specific T-cell repertoires. The FEST (Functional Expansion of Specific T cells) assay described herein integrates T-cell receptor sequencing of short-term, peptide-stimulated cultures with a bioinformatic platform to identify antigen-specific clonotypic amplifications. This assay can be adapted for all types of antigens, including MANAs via tumor exome-guided prediction of MANAs. Following *in vitro* identification by the MANAFEST assay, the MANA-specific CDR3 sequence can be used as a molecular barcode to detect and monitor the dynamics of these clonotypes in blood, tumor, and normal tissue of patients receiving immunotherapy. MANAFEST is compatible with high-throughput routine clinical and lab practices. *Cancer Immunol Res; 6(8); 888–99. ©2018 AACR.*

## Introduction

Patients can mount endogenous immune responses against mutation-associated neoantigens (MANA), but these responses are countered by immunosuppressive signals—so-called checkpoints (1). Unleashing of MANA-specific T cells by checkpoint blockade promotes tumor regression in patients who achieve clinical responses (2). Sensitive and specific T-cell assays that assess the repertoire of MANA-specific T cells are needed to understand the nature of antitumor immunity and to identify biomarkers predictive of response to immunotherapies. Current immunologic approaches identify antigen recognition and memory T-cell responses by assaying effects downstream of T-cell receptor (TCR) engagement through cytotoxic T-cell assays, polyfunctional intracellular cytokine staining (ICS), or ELISpot (3). Antigen-specific T cells, regardless of effector function or cytokine production, can be identified using peptide:MHC multimer-based flow cytometry. These immune assays operate with low sensitivity or rely on production of specific cytokines for antigen recognition to be detected. Under ideal conditions, ELISpot can detect as few as 4 cytokine-secreting cells per 100,000 peripheral blood mononuclear cells (PBMC; ref. 4), but sensitivity is frequently limited by high backgrounds. ICS can detect 1 cytokine-secreting cell in 10,000 (5), and multimers can identify 1 in 5,000 antigen-specific T cells (6, 7).

However, when evaluating responses to tumor-associated antigens (TAA) or MANAs, to which T cells could have been primed in an environment of tolerance rather than the inflammatory environment induced by viruses, these conventional antigen detection assays are insufficient. A tandem mini gene (TMG) approach has been described that can evaluate T-cell recognition of up to 16 genes in a given T-cell culture after expansion (8, 9). Although this method has increased the number of genes that can be evaluated for immunologic recognition, it utilizes IFNγ ELISpot and/or 4-1BB upregulation as the readout. A method developed by Schumacher and colleagues allows for the analysis of >28 MANAs simultaneously in a single sample using a combinatorial barcoded multimer approach (10). However, the TMG-based approach and combinatorial multimer encoding are technically challenging

[1]The Bloomberg-Kimmel Institute for Cancer Immunotherapy, Johns Hopkins University School of Medicine, Baltimore, Maryland. [2]The Sidney Kimmel Comprehensive Cancer Center, Johns Hopkins University School of Medicine, Baltimore, Maryland. [3]Vavilov Institute of General Genetics, Russian Academy of Sciences, Moscow, Russia. [4]Department of Pathology, Johns Hopkins University School of Medicine, Baltimore, Maryland.

**Note:** Supplementary data for this article are available at Cancer Immunology Research Online (http://cancerimmunolres.aacrjournals.org/).

L. Danilova and V. Anagnostou contributed equally to this article.

F. Housseau and K.N. Smith contributed equally to this article.

**Corresponding Author:** Kellie N. Smith, Johns Hopkins University School of Medicine, CRB-I Room 4M51, 1650 Orleans Street, Baltimore, MD 21287. Phone: 410-502-7523; Fax: 410-614-0549; E-mail: kellie@jhmi.edu

**doi:** 10.1158/2326-6066.CIR-18-0129

and not yet high throughput or compatible with routine clinical monitoring of the antitumor immune response. Based on these conventional assays, investigators have concluded that only a small number (generally <4) of potential MANAs are recognized in a given cancer patient, even when there are hundreds identified by prediction algorithms in cancers with high mutational burden. A question remains as to whether the repertoire of functional MANA-specific T cells is in fact that limited or whether existing assays are not sensitive enough to identify larger repertoires.

Beyond the detection of antigen-specific T cells, high-throughput molecular approaches are needed to routinely measure the breadth of the TAA- and MANA-specific TCR repertoire in cancer patients and monitor their response to immunotherapy. Although not all cells secrete enough cytokines to be detected by current assays, the response of all T cells upon recognition of their cognate antigen is clonal expansion (11, 12), even in cases of tolerance induction or exhaustion (13). T cells recognize antigen through engagement of the TCR with a unique cognate peptide:MHC complex. High diversity in complementarity-determining region 3 (CDR3), which is responsible for peptide:MHC recognition, enables the body to mount immunity against a range of peptide antigens and is the basis of T-cell antigen specificity. Advances in sequencing of the TCR CDR3 region and quantification of TCRVβ clonotypes (14, 15) have enabled tracking of T-cell clones in peripheral blood, T-cell cultures, formalin-fixed paraffin-embedded (FFPE) tissue, and/or fresh-frozen tissue. However, analysis of CDR3 regions does not provide information on antigen specificity. We therefore developed the functional expansion of specific T cells (FEST) assays that use TCRseq to analyze antigen-specific clonal expansion. In conjunction, we developed a web-based bioinformatics platform to characterize expanded antigen-specific TCR Vβ clonotypes. These assays can be done with peptides representing candidate viral antigens (ViraFEST, which we used to optimize simple one-step culture variables), TAAs (TAAFEST), or MANAs (MANAFEST). The FEST assays are based on TCR clonotypic quantification in a set of short-term peptide-stimulated T-cell cultures and function independently of cytokine production. The FEST platform can work with all HLA haplotypes and allows for tracking of antigen-specific T cells in FFPE and/or frozen tissue based on the ability of CDR3 regions to be used as a barcode for clones whose specificity is defined in the FEST assay.

We show that the MANAFEST assay, supported by a web-based analytic platform, identifies MANA-specific TCR Vβ clones that can be matched with clones detected in tumor tissue and in the blood of cancer patients treated with checkpoint blockade. MANAFEST can therefore validate the tumor specificity of TCR Vβ clonotypes, interrogate the dynamics of the antigen-specific T-cell response over time, and monitor the efficacy of checkpoint blockade using liquid biopsies obtained before or after treatment. The FEST assays can detect antigen-specific T-cell responses with sensitivity, specificity, and high throughput.

## Materials and Methods

### Healthy donors and patients

This study was approved by the institutional review board (IRB) of Johns Hopkins University (JHU) and was conducted in accordance with the Declaration of Helsinki and the International Conference on Harmonization Good Clinical Practice guidelines. The healthy donors and patients described in this study provided written informed consent as approved by the IRB of Johns Hopkins University. Patient JH124 was diagnosed with stage IIB squamous non–small cell lung cancer (NSCLC) in November 2015 and was enrolled on JHU IRB protocol NA_00092076 at the Sidney Kimmel Comprehensive Cancer Center. He received 2 doses of anti–PD-1 immunotherapy and underwent surgical resection in December 2015 (16). Pathology demonstrated a complete pathologic response in the 9-cm primary tumor and N1 nodes positive for tumor; final pathology stage was IIA. The patient received adjuvant platinum-based chemotherapy from February 2016 to May 2016. He has no evidence of recurrence of his cancer at last follow-up in December 2017.

### Whole-exome sequencing and putative MANA identification

Whole-exome sequencing of matched tumor–normal samples and identification of candidate neoantigens was performed as previously described using the VariantDx and ImmunoSelect-R pipelines (Personal Genome Diagnostics; refs. 17, 18). Briefly, the pretreatment tumor sample underwent pathologic review for confirmation of lung cancer diagnosis and assessment of tumor purity. Slides from the FFPE block were macrodissected to remove contaminating normal tissue and peripheral blood was used as matched normal. DNA was extracted from tumor and matched peripheral blood using the Qiagen DNA FFPE and Qiagen DNA blood mini kit, respectively (Qiagen). Fragmented genomic DNA from tumor and normal samples was used for Illumina TruSeq library construction (Illumina) and exonic regions were captured in solution using the Agilent SureSelect v.4 kit (Agilent) according to the manufacturer's instructions as previously described (17–20). Paired-end sequencing, resulting in 100 bases from each end of the fragments for the exome libraries, was performed using Illumina HiSeq 2000/2500 instrumentation (Illumina). Depth of coverage was 209× and 80× for the tumor and matched normal, respectively.

### Primary processing of next-generation sequencing data and identification of putative somatic mutations

Somatic mutations were identified using the VariantDx custom software for identifying mutations in matched tumor and normal samples as previously described (18). In brief, prior to mutation calling, primary processing of sequence data for both the tumor and normal sample was performed using Illumina CASAVA software (version 1.8), including masking of adapter sequences. Sequence reads were aligned against the human reference genome (version hg19) using ELAND with additional realignment of select regions using the Needleman–Wunsch method (21). Candidate somatic mutations, consisting of point mutations, insertions, and deletions were then identified using VariantDx across the whole exome. VariantDx examines sequence alignments of tumor samples against a matched normal while applying filters to exclude alignment and sequencing artifacts. In brief, an alignment filter was applied to exclude quality failed reads, unpaired reads, and poorly mapped reads in the tumor. A base-quality filter was applied to limit inclusion of bases with reported Phred quality score > 30 for the tumor and > 20 for the normal. A mutation in the pre- or post-treatment tumor samples was identified as a candidate somatic mutation only when (i) distinct paired reads contained the mutation in the tumor; (ii) the fraction of distinct paired reads containing a particular mutation in the tumor was at least 10% of the total distinct read pairs; and (iii) the mismatched base was not present in >1% of the reads in the matched normal

sample as well as not present in a custom database of common germline variants derived from dbSNP and (iv) the position was covered in both the tumor and normal. Mutations arising from misplaced genome alignments, including paralogous sequences, were identified and excluded by searching the reference genome. Our mutation calling algorithm specifically removes changes that are present at very low levels, enabling characterization of *bona fide* somatic genomic alterations.

Candidate somatic mutations were further filtered based on gene annotation to identify those occurring in protein-coding regions. Functional consequences were predicted using snpEff and a custom database of CCDS, RefSeq, and Ensembl annotations using the latest transcript versions available on hg19 from UCSC (22). Predictions were ordered to prefer transcripts with canonical start and stop codons and CCDS or RefSeq transcripts over Ensembl when available. Finally, mutations were filtered to exclude intronic and silent changes, while retaining mutations resulting in missense mutations, nonsense mutations, frameshifts, or splice site alterations. A manual visual inspection step was used to further remove artifactual changes.

**Neoantigen predictions**

To assess the immunogenicity of somatic mutations, exome data combined with the patient's MHC class I haplotype were applied in a neoantigen prediction platform that evaluates binding of somatic peptides to class I MHC, antigen processing, self-similarity, and gene expression. Detected somatic mutations, consisting of nonsynonymous single-base substitutions, insertions, and deletions, were evaluated for putative neoantigens using the Immuno*Select*-R pipeline (Personal Genome Diagnostics). To accurately infer the germline HLA 4-digit allele genotype, whole-exome-sequencing data from paired tumor/normal samples were first aligned to a reference allele set, which was then formulated as an integer linear programming optimization procedure to generate a final genotype (23). The HLA genotype served as input to netMHCpan to predict the MHC class I binding potential of each somatic and wild-type peptide ($IC_{50}$ nmol/L), with each peptide classified as a strong binder (SB), weak binder (WB), or nonbinder (NB; refs. 24–26). Peptides were further evaluated for antigen processing by netCTLpan (27) and were classified as cytotoxic T lymphocyte epitopes (E) or nonepitopes (NA). Paired somatic and wild-type peptides were assessed for self-similarity based on MHC class I binding affinity (28). Neoantigen candidates meeting an $IC_{50}$ affinity < 500 nmol/L were subsequently ranked based on MHC binding and T-cell epitope classifications. Tumor-associated expression levels derived from TCGA were used to generate a final ranking of candidate immunogenic peptides. Putative MANAs were synthesized using the PEPscreen platform (Sigma-Aldrich). Lyophilized peptides were dissolved in minimal DMSO, resuspended in 100 μg/mL aliquots in AIM V media, and stored at −80°C.

**T-cell culture**

T cells were cultured and evaluated for antigen-specific expansions as previously described, with minor modifications (16, 17, 29). Briefly, on day 0, frozen PBMCs from healthy donors or patients were thawed and counted. T cells were isolated using the EasySep Human T Cell Enrichment Kit (Stemcell Technologies). T cells were washed, counted, and resuspended at $2.0 \times 10^6$/mL in AIM V media supplemented with 50 μg/mL gentamicin (ThermoFisher Scientific). The T cell–negative fraction was washed, counted, and irradiated at 3,000 γ-rads. The irradiated T cell–depleted fraction was washed and resuspended at $2.0 \times 10^6$/mL in AIM V media supplemented with 50 μg/mL gentamicin. Irradiated T cell–depleted cells were added to a 96-well, 48-well, 24-well, or 12-well plate at 125, 250, 500, or 1,000 μL per well, respectively. An equal volume of T cells was then added to each well, along with 1 μg/mL of one of 13 HLA-matched CMV, EBV, or flu peptide epitopes (Sigma-Aldrich) or without peptide. Cells were cultured for 10 days at 37°C in a 5% $CO_2$ atmosphere, replacing half the culture media with fresh culture media containing 100 IU/mL IL2, 50 ng/mL IL7, and 50 ng/mL IL15 (for final concentrations of 50 IU/mL IL2, 25 ng/mL IL7, and 25 ng/mL IL15) on day 3 and replacing half the culture media with fresh media containing 200 IU/mL IL2, 50 ng/mL IL7, and 50 ng/mL IL15 (for final concentrations of 100 IU/mL IL2, 25 ng/mL IL7, and 25 ng/mL IL15) on day 7. If cells were to be used in IFNγ ELISpot or IFNγ/granzyme B fluorospot assays, cells were rested on day 9 by removing half the media and replacing with fresh media without cytokines. For cells to be used in TCR sequencing/FEST analysis, cells were not rested and were harvested on day 10. $CD8^+$ cells were further isolated from T cells cultured with putative MANAs using the EasySep Human $CD8^+$ T Cell Enrichment Kit (Stemcell Technologies) and plate magnet for added throughput.

For the generation of 20-day, restimulated cultures, autologous PBMCs were incubated with 1 μg/mL relevant peptide for 2 hours at 37°C in a 5% $CO_2$ atmosphere, irradiated at 3,000 γ-rads, and were added to cultures at a 1:1 T cell:PBMC ratio on day 10 of the culture. Cells were fed on culture days 13 and 17 by replacing half the culture media with fresh media containing 200 IU/mL IL2, 50 ng/mL IL7, and 50 ng/mL IL15 (for final concentrations of 100 IU/mL IL2, 25 ng/mL IL7, and 25 ng/mL IL15). On day 20, T cells were harvested and washed for DNA extraction.

**Staining and sorting of pentamer-positive populations**

T cells obtained from healthy donors were evaluated for specificity of known viral antigens. Fluorochrome-conjugated pentamers were synthesized (ProImmune) and used to stain PBMCs from healthy donor JH014 per the manufacturer's instructions. Cells were costained with CD3, CD4, CD8, and CD45RO to identify antigen-specific memory $CD8^+$ T cells for sorting. The pentamer-positive population of interest was sorted using a BD FACSAria II and DNA was immediately extracted for TCR sequencing.

**TCR sequencing and assessment of antigen-specific expansions**

DNA was extracted from peptide-stimulated T cells, tumor tissue, and longitudinal pre- and posttreatment PBMCs and pentamer-sorted T cells using a Qiagen DNA blood mini kit, DNA FFPE kit, or DNA blood kit, respectively (Qiagen). TCR Vβ CDR3 sequencing was performed using the survey (tissue, cultured cells, and pentamer-sorted cells) or deep (PBMC) resolution Immunoseq platforms (Adaptive Biotechnologies; refs. 14, 15). Clonotypes were considered to be expanded if their abundance was significantly higher in the relevant peptide-stimulated T cell culture relative to T cells cultured without peptide using Fisher exact test with Benjamini–Hochberg correction for false discovery rate (FDR; $P < 0.05$).

**IFNγ ELISpot assays**

10-day cultured cells or uncultured PBMCs obtained from the same stock of cells used in culture were evaluated for IFNγ production by a standard overnight enzyme-linked immunosorbent spot (ELISpot) assay. Briefly, 96-well nitrocellulose plates (EMD Millipore) were coated with anti-IFNγ monoclonal antibody (10 μg/mL; Mabtech) and incubated overnight at 4°C. Plates were washed and blocked with IMDM supplemented with 10% heat-inactivated FBS for 2 hours at 37°C. T cells stimulated for 10 days with CMV, EBV, and flu peptides were added to wells in duplicate at 50,000 cells per well and were stimulated overnight with PBMCs preloaded with 1 μg/mL relevant peptide, a cytomegalovirus (CMV), Epstein–Barr virus (EBV), and influenza virus peptide pool (CEF), or no peptide in AIM V media. Cultured T cells with PBMCs alone served as the background/negative control condition. Fresh-thawed PBMCs were added to wells in singlet at 100,000 cells/well and were stimulated overnight with 1 μg/mL of the same peptides used in the T-cell culture assays. PBMCs alone in duplicate wells served as the background/negative control condition.

**Bioinformatic analysis**

We developed a custom script in R/Bioconductor (30, 31) to load TCR sequencing data exported from Adaptive Biotechnologies ImmunoSEQ platform in V2 in the tab-delimited format, perform the analysis, and visualize and save results. For analysis, we used only productive clones and summarized template counts for nucleotide sequences that translated into the same amino acid sequence. For each clone, we applied Fisher exact test to compare the number of templates in a culture of interest (with peptide) and a reference culture (without peptide). The *P* value adjusted by Benjamini–Hochberg procedure (FDR; ref. 32) was used to determine antigen-specific clonotypes (FEST assay–positive clones) that met the following criteria: (i) expanded in the culture of interest compared with the reference culture (T cells cultured with cytokines but without peptide) at an FDR less than the specified threshold (<0.05; default value), (ii) expanded in the culture of interest compared with every other culture performed in tandem (FDR < 0.05; default value), (iii) have an odds ratio >5 (default value), and (iv) a minimum template threshold in uncultured T cells calculated by:

$$\text{limit} = 1 - (1 - P)^{(1/n)}$$

where *P* is the probability of observing the clone in a given well (clone confidence) and *n* is the estimated number of $CD8^+$ T cells per well prior to culture (default value is 100,000). All clones were subject to a 10-template lower threshold for consideration in the statistical analysis. FEST assay–positive clones were saved in the output table and plotted as an output heat map using build-in R functions. The script was wrapped into a web application using Shiny Server (33). This web application is publicly available at http://www.stat-apps.onc.jhmi.edu/FEST and the source code has been deposited at https://sourceforge.net/projects/manafest/.

## Results

***In vitro* TCRVβ CDR3 clonotype amplification as a functional readout of T-cell recognition**

To validate TCR Vβ clonotypic amplification as a metric of T-cell recognition, we first evaluated T-cell responses in a healthy donor to common viral antigens and compared IFNγ ELISpot with TCRseq in healthy donors. Cytomegalovirus (CMV)-, influenza (flu)-, and EBV-derived HLA-I epitopes are well-defined and induce $CD8^+$ T-cell responses detectable by IFNγ. We therefore used ELISpot as a reference assay for the technical validation of FEST. We initially tested if peptide-induced T-cell expansion could be observed in the absence of ELISpot positivity (no detectable antigen-specific IFNγ). We cultured T cells from healthy donor JH014 for 10 days with multiple HLA-matched viral peptide epitopes (Supplementary Table S1) or no peptide as a control. At the term of the culture, one aliquot of the cells was used to perform IFNγ ELISpot and the remaining cells were evaluated by TCRseq for significant clonotypic expansions (FDR < 0.05; see Materials and Methods) relative to the control. Mean antigen-specific IFNγ production of >6,000 spot-forming cells (SFC) per $10^6$ PBMCs was associated with expansion of 47 and 130 T-cell clonotypes after culture with the HLA A11-restricted EBV EBNA 4NP (4NP, Fig. 1A; Supplementary Table S2) and HLA B8-restricted EBV EBNA 3A epitopes (3A, Fig. 1B; Supplementary Table S2), respectively. Although there was no IFNγ ELISpot signal for the HLA A11-restricted EBV 1 epitope, 87 T-cell clonotypes showed expansion by TCRseq analysis (Fig. 1C; Supplementary Table S2). Therefore, TCRseq can not only be used to detect an antigen-specific response after a 10-day peptide stimulation, but it can quantitatively analyze the polyclonality of the response, which is not achievable with ELISpot.

**Validation of the specificity of expanded clonotypes by multimer staining**

To validate that expanded clonotypes detected by TCRseq are specific for the peptide used in the culture, we first evaluated the nature of the 4NP-specific repertoire in healthy donor JH014 by sorting and performing TCRseq on pentamer-positive ($pMHC^+$) $CD8^+$ T cells. The 4NP-specific $CD8^+$ T cells represented 0.2% of total uncultured T cells (baseline; Fig. 2A). TCRseq of these $pMHC^+$ T cells demonstrated dominance of Vβ 28-01 within this antigen-specific population (Fig. 2B; Supplementary Table S3), which is consistent with prior findings that different T-cell clonotypes specific for the same antigen often utilize the same Vβ gene segment (34–38). In comparison with 92.5% of T cells utilizing Vβ 28-01 in $pMHC^+$ T cells, only 7.0% of $pMHC^-$ $CD8^+$ T cells used this gene segment (Supplementary Table S4). These findings were recapitulated after a 10-day culture, whereby $pMHC^+$ T cells made up 15.6% of the T-cell population, and the Vβ 28-01 gene segment was utilized by 97.3% of $pMHC^+$ T cells (Fig. 2B; Supplementary Table S3). We then compared the pMHC-specific CDR3 Vβ sequences with those amplified in bulk T cells after a 10-day culture and stimulation with the 4NP epitope (as reported in Fig. 1; Supplementary Table S2). Four unique clones matched $pMHC^+$ CDR3 Vβ sequences (Table 1).

We also performed this analysis on EBV EBNA 3A-$pMHC^+$ T cells. At baseline, 0.3% of T cells were $pMHC^+$ and 89.3% of these used the Vβ 06-06 gene segment (Fig. 3A; Supplementary Table S5). After a 10-day peptide stimulation, 4.6% of T cells were $pMHC^+$ and only 18.4% of these used Vβ 06-06, with Vβ 04-03 becoming the dominant gene segment in this population (Fig. 3B; Supplementary Table S5). Five $pMHC^+$ clonotypes matched expanded clonotypes as reported in Fig. 1; Supplementary Table S2; one of these was detected by pentamer only after the 10-day culture (Table 2), and there was no preferential use of any Vβ gene segment among $pMHC^+$ cells.

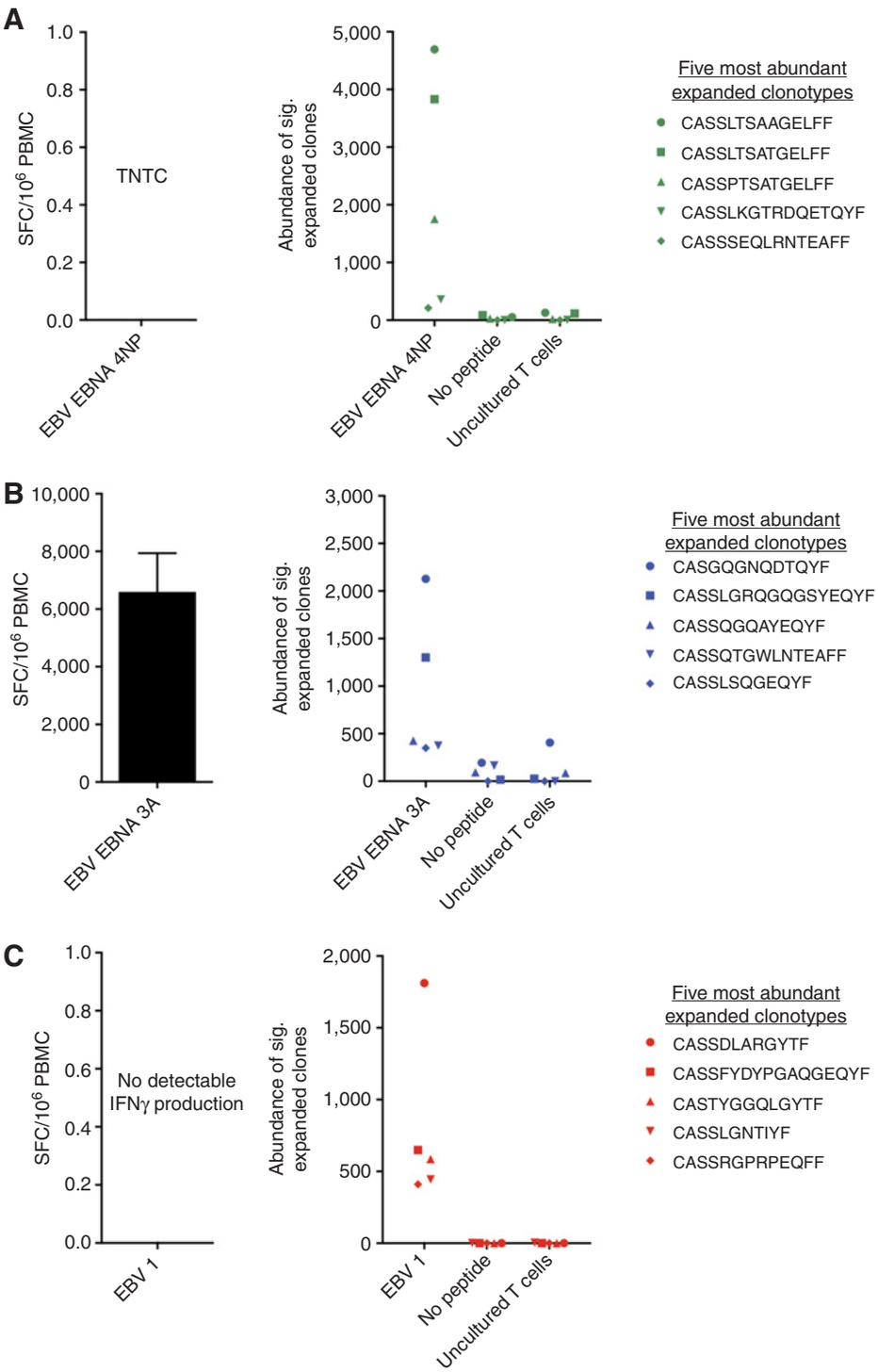


**Figure 1.**
IFNγ ELISpot underestimates the breadth of the antigen-specific T-cell response. T cells from healthy donor JH014 were stimulated with one of 13 known MHC class I–restricted epitopes (Supplementary Table S1) and cultured for 10 days. IFNγ ELISpot was performed in duplicate wells on an aliquot of cultured T cells (left) and TCR Vβ CDR3 sequencing was performed on the remaining T cells, T cells cultured without peptide, and uncultured T cells (right). ELISpot data are shown as the mean number of spot-forming cells (SFC) per $10^6$ cells with background subtracted for 3 tested epitopes. Accompanying significant expansions (Fisher exact test with Benjamini–Hochberg correction for FDR, <0.05) of the 5 clonotypes with the highest abundance postculture are also shown in response to these 3 epitopes, 4NP (**A**, green), 3A (**B**, blue), and EBV 1 (**C**, red). Each symbol represents a unique CDR3 clonotype. The full list of significantly expanded clones is shown in Supplementary Table S2. ELISpot background is the mean number of SFC detected without peptide stimulation in the ELISpot plus two standard deviations. TCR sequencing data are shown as the number of templates of each clone (abundance) that was detected in the relevant condition. TNTC, too numerous to count.

These findings validate the use of TCRseq and the quantification of TCR Vβ clonotypic amplification as a method to identify antigen-specific T cells among PBL and suggest that Vβ gene dominance after a 10-day culture is insufficient to identify an antigen-specific T-cell response.

### Sensitivity of TCRseq for detecting antigen-specific T-cell clonotype expansion

The TCRseq-based approach described here relies on the identification of antigen-specific Vβ CDR3 clonotypes and on their frequency following a 10-day *in vitro* expansion. Sensitivity of this

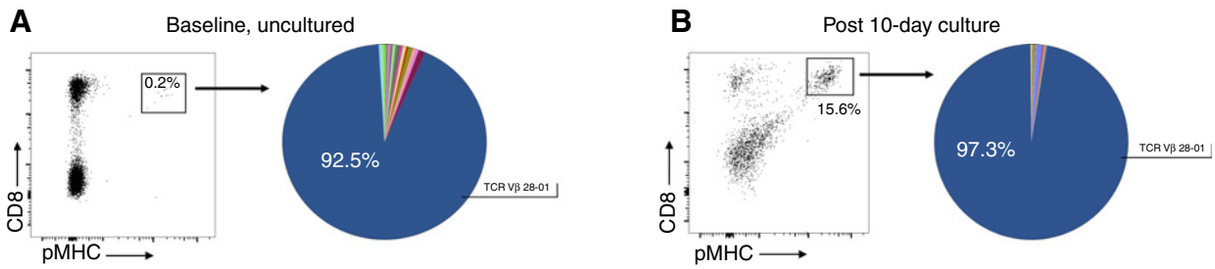


**Figure 2.**

Validation of expanded clonotypes specific for 4NP. 4NP pMHC$^+$ T cells from donor JH014 were sorted by FACS prior to culture (**A**, left) or after a 10-day stimulation with the EBV EBNA 4NP epitope (**B**, left). TCR Vβ CDR3 sequencing was performed on the pMHC$^+$ population and the Vβ gene segment usage was evaluated (**A** and **B**, right). The full list of clonotypes and their representation within the pMHC$^+$ population are shown in Supplementary Table S3. Clonotypes identified in the pentamer-sorted population were compared with those found in the same peptide-stimulated 10-day culture. Outgrowth of these clones was detected in 5 separate experiments.

approach (i.e., the detection of low-frequency clonotypes) is expected to be dependent on the starting number of CD8$^+$ T cells in the 10-day culture and could be affected by the concentration of peptide used in the stimulation. We therefore sought to determine (i) the optimal number of starting T cells required to capture the breadth of the antigen-specific repertoire and (ii) the lower limit peptide concentration that could induce detectable antigen-specific T-cell expansion. We first cultured titrating numbers of T cells (from $1.25 \times 10^5$ to $1.0 \times 10^6$) obtained from two healthy donors for 10 days. T cells from donor JH014 and JH016 were stimulated with the HLA A11-restricted 4NP and the HLA A2-restricted influenza M peptide epitopes, respectively (Supplementary Table S1). Peptide epitopes were chosen based on previously documented reactivity in these two donors. In both donors, the number of unique clonotypes that expanded relative to the "no peptide" control decreased as the starting cell number was decreased (Fig. 4A). Therefore, a higher number of cultured cells will result in the identification of a higher number of unique antigen-specific clonotypes.

The aggregate number of productive reads corresponding to expanded clonotypes decreased when reducing the starting cell number (Fig. 4B). These findings show that the number of T cells used per well influences the diversity (number of unique TCR clonotypes) and enrichment (frequency of each clonotype) of the antigen-specific repertoire after culture. Indeed, there was a correlation between the percentage of total productive reads that were expanded and the clonality metric of the cultures ($P = 0.02$, $r^2 = 0.61$; Fig. 4C), showing that clones expanded and detected via TCRseq contribute to the clonality of the culture. These findings highlight the ability of the 10-day peptide-stimulated culture to enrich for antigen-specific T cells. Despite the observance of more unique clones and a higher abundance of expanded clones when culturing $1 \times 10^6$ T cells, clones were still expanded in all peptide cultures even at the lowest starting cell number of $1.25 \times 10^5$. Therefore, a 10-day culture with as few as $1.25 \times 10^5$ starting T cells per condition is sufficient to screen a library of peptides for recognition of peripheral T cells with frequencies as low as 0.0008% (1 cell in 125,000), with the sensitivity increasing to 0.0001% when starting with $1.0 \times 10^6$ T cells (1 cell in $1.0 \times 10^6$). Titration of the 4NP peptide in donor JH014 demonstrated the ability to detect expansions via TCRseq and expansion of pMHC-matched clonotypes at concentrations as low as 1 ng/mL (Fig. 4D and E).

We next assessed the possibility that a 10-day restimulation following the initial culture could reveal memory T-cell responses that were undetectable on day 10. T cells from healthy donor JH014 were cultured with two HIV-1 (SL9 and TV9) and one Ebola HLA A*02:01-restricted peptide (AY9) epitopes. After 10 days, one expanded clonotype was detected in response to the HIV-1 gag p24 epitope, TV9 (Supplementary Fig. S1 and Supplementary Table S6). No clonotypes were expanded in response to the other two epitopes tested. After a restimulation and 20 days of culture, there was expansion of 90, 137, and 147 clones in response to the HIV-1 gag SL9, HIV-1 gag TV9, and ebolavirus AY9 epitopes, respectively (Supplementary Fig. S1 and Supplementary Table S6). These data suggest that a restimulation and 20-day culture can result in the detection of primary T-cell responses and is therefore not suitable when evaluating the endogenous memory repertoire, but may inform on the repertoire that is available for vaccination.

### FEST-associated bioinformatic platform

We report here the expansion of multiple clonotypes in response to viral antigens. Although several of these clonotypes have been validated by pentamer staining (Figs. 2 and 3), some were nonetheless expanded in response to other viral antigens tested (Supplementary Table S2). Indeed, the sensitivity of our TCRseq-based approach might be associated with low specificity and a high false-positive rate. To ensure the specificity of clones expanded in culture and minimize false positives, we developed a publicly available high-throughput statistical analysis platform

**Table 1.** Gene usage and frequency of EBV EBNA 4NP pMHC$^+$-matched clonotypes

| pMHC$^+$-matched clonotypes | Dominant Vβ gene usage | Frequency in EBV EBNA 4NP pMHC$^+$ population (%) | | Frequency among bulk T cells (%) | |
|---|---|---|---|---|---|
| | | Baseline, uncultured | Post 10-day culture | Baseline, uncultured | Post 10-day culture |
| CASSLTSATGELFF | 28-01*01, 17-01*01 | 43.98 | 31.48 | 0.13 | 17.31 |
| CASSLTSAAGELFF | 28-01*01 | 37.65 | 33.83 | 0.14 | 21.21 |
| CASSPTSATGELFF | 28-01*01, 03 | 7.79 | 20.06 | 0.02 | 7.93 |
| CASSLKGTRDQETQYF | 28-01*01 | 0.58 | 10.78 | 0.01 | 1.63 |

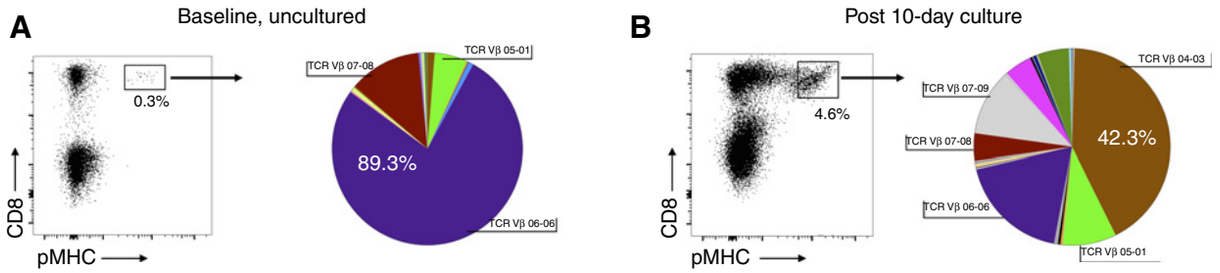


**Figure 3.**

Validation of expanded clonotypes specific for 3A. 3A pMHC$^+$ T cells from donor JH014 were sorted by FACS prior to culture (**A**, left) or after a 10-day stimulation with the EBV EBNA 3A epitope (**B**, left). TCR Vβ CDR3 sequencing was performed on the pMHC$^+$ population, and the Vβ gene segment usage was evaluated (**A** and **B**, right). The full list of clonotypes and their representation within the pMHC$^+$ population are shown in Supplementary Table S4. Clonotypes identified in the pentamer-sorted population were compared with those found in the same peptide-stimulated 10-day culture.

that integrates each clonotypic amplification in a set of peptide-stimulated cultures to determine the positivity and specificity of antigen-specific T-cell recognition (http://www.stat-apps.onc.jhmi.edu/FEST).

For confidence in antigen-specificity, a clonotype should first meet a minimum frequency threshold in uncultured CD8$^+$ T cells; this threshold is implemented to ensure sufficient representation of the clone in the majority of wells prior to culture and is calculated by integrating a user-defined level of confidence with the estimated number of CD8$^+$ T cells per well (see Materials and Methods). Additionally, after culture, this clonotype should (i) be significantly expanded in the relevant culture compared to T cells cultured without peptide at a false discovery rate (FDR) <0.05, (ii) be significantly expanded in the relevant culture compared to T cells cultured with every other peptide at FDR < 0.05, and (iii) have an odds ratio (OR) >5 compared with the "no peptide" control. These recommended criteria, in addition to a template threshold, can be adjusted on the user interface according to user preference and experimental setup to minimize false positives in light of the sensitivity of the assay platform. In our analyses below, clones satisfying these criteria were considered to be viral- or MANA-specific and were saved as an output of analysis (Supplementary Data S1). In addition to identification of antigen-specific clonotypes, the FEST platform permits inclusion of TCRseq data from samples that are not involved in the analysis to identify antigen-specific clonotypes but are of interest for tracking these clonotypes in biological compartments, such as peripheral blood and tissue. A heatmap is also generated in the analysis platform to document all significantly expanded clones detected across all cultures and to cluster clonotypes based on expansion relative to the control.

The statistical specificity of each T-cell clone for a given peptide is controlled by every other peptide culture, with each one representing an additional negative control. Accordingly, our confidence in the specificity of T-cell recognition can be improved by increasing the number of distinct peptide cultures. With 46 cultures, the estimated specificity of a unique clonotype would be nearly 98% (45/46), and a one-sided 95% confidence interval (CI) would run from 90% to 100%. Therefore, with at least 46 cultures we can be 95% confident that specificity is above 90%. With 93 cultures, a unique clonotype has an estimated specificity of approximately 99% (95% CI = 95%–100%). The FEST assays, comprised of an experimental T-cell culture and computerized analytical tool, therefore allows us to monitor and analyze antigen-specific T-cell responses in a high-throughput fashion in patients with all HLA alleles independently of cytokine production and laborious readout assays.

When we applied the FEST analysis as described above to the experiments described in Fig. 1, five unique 4NP-specific clonotypes were detected, which included the four clonotypes detected in the pMHC$^+$ population (pMHC$^+$-matched) shown in Fig. 2C (Supplementary Data S1). Of the total number of templates (equivalent to number of cells) after sequencing, 99.7% corresponded to these pMHC$^+$-matched clones. This analysis platform detected no specific responses when comparing five identical replicate cultures stimulated with the 4NP peptide, despite significant expansion of the pMHC$^+$-matched clonotypes relative to the "no peptide" control. This demonstrates the power of our test in discriminating a true antigen-specific response. The single clonotype that was positive by the FEST assay but not detected by pMHC (Supplementary Data S1) represented 0.15% of cultured T cells. This therefore suggests the FEST platform can capture

**Table 2.** Gene usage and frequency of EBV EBNA 3A pMHC$^+$-matched clonotypes

| pMHC$^+$-matched clonotypes | Vβ gene usage | Frequency in EBV EBNA 3A pMHC$^+$ population (%) | | Frequency among bulk T cells (%) | |
|---|---|---|---|---|---|
| | | Baseline, uncultured | Post 10-day culture | Baseline, uncultured | Post 10-day culture |
| CASGQGNQDTQYF | 06-06, 06-09*01, 06-05*01, 06-07*01, 10-03*01, 06-04, 06-08*01 | 77.78 | 18.82 | 0.45 | 8.17 |
| CASSQGQAYEQYF | 07-08*01, 07-04*01, 07-03*01, 07-02*01, 07-07*01, 11-03*01, 11-02*02, 07-01*01 | 12.08 | 4.80 | 0.10 | 1.64 |
| CASSLGRQGQGSYEQYF | 05-01*01, 04-03*01 | 5.31 | 8.46 | 0.03 | 5.00 |
| CASSPTRGFGGEQFF | 04-03*01, 05-05*01, 05-08*01, 11-02*02, 07-09, 11, 05-04*01, 04-01*01, 05-02*01, 07-02*01, 05-01*01, 07-08*01, 05-03 | 0.72 | 38.24 | 0.00 | 0.82 |
| CASILRTSGYANTGELFF | 28-01*01 | 0.00 | 5.01 | 0.00 | 0.34 |

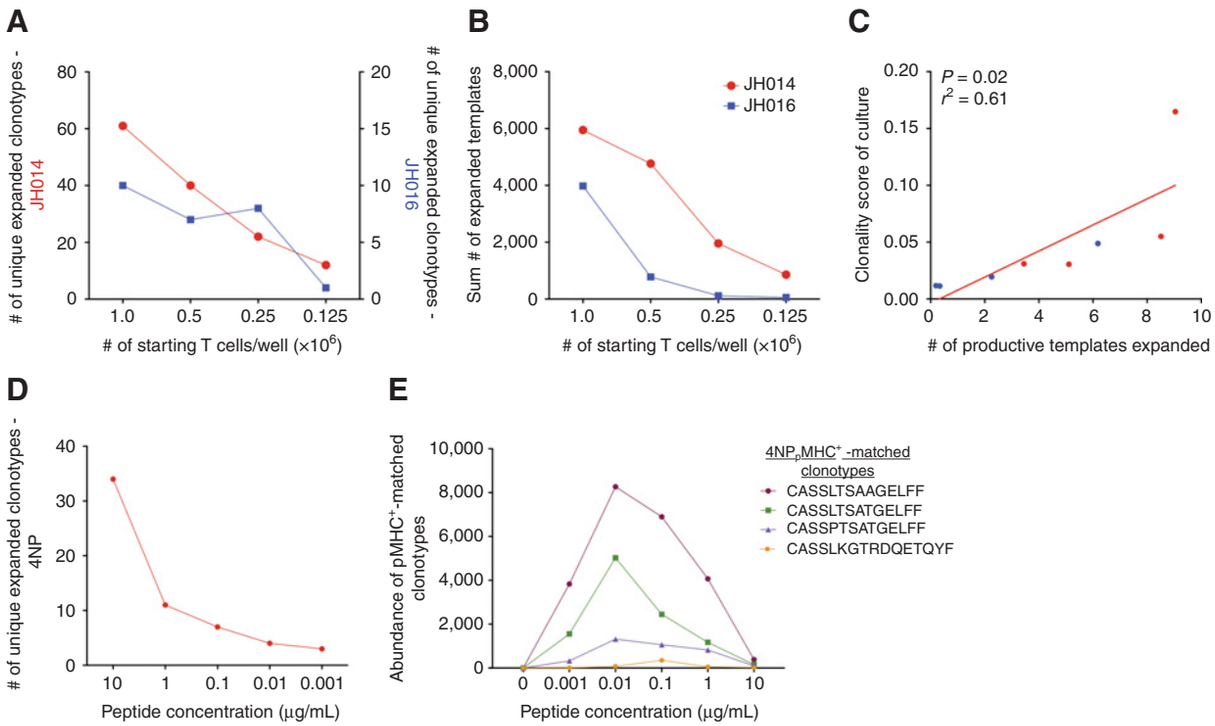


**Figure 4.**

FEST assay sensitivity. Titrating numbers of T cells from healthy donors JH014 (red) and JH016 (blue) were stimulated with the A11-restricted 4NP and the A2-restricted flu M peptide epitopes (Supplementary Table S1), respectively, for 10 days. Clonotypes significantly expanded relative to the "no peptide" control were identified in each condition. **A,** The number of unique clonotypes that were expanded, as well as **(B)** the total number of templates corresponding to these clonotypes, is shown for each titrating cell number. **C,** The correlation between clonality and the percentage of productive templates that were expanded after the 10-day culture is shown. Additionally, T cells from donor JH014 were stimulated for 10 days with titrating concentrations of the 4NP peptide epitope. Data are reported as **(D)** the number of unique expanded clonotypes detected at each concentration or **(E)** the number of templates detected for each of the four pMHC$^{+}$-matched clonotypes (abundance).

lower frequency clonotypes that would require large numbers of cells or high pMHC affinity to be detected by multimer staining. The 3A epitope induced no responses as determined by the FEST assay. Upon further interrogation, the 5 pmol/LHC$^{+}$-matched clones shown in Table 2 were also significantly expanded (FDR < 0.05) with an OR > 5 in response to the A2-restricted EBV BMLF1 epitope (Supplementary Table S1). The 3A epitope, FLRGRAYGL, and the BMLF1 epitope, GLCTLVAML, share the leucine anchor residues at positions 2 and 9 commonly seen in A*0201-restricted epitopes (39, 40). Despite being identified as a B8-restricted epitope, 3A is also predicted to bind A*02:01 with weak affinity (0.85% rank, netMHCpan). Amino acid composition analysis suggests the two peptide epitopes have similarities in nonpolarity and acidity. For this reason, we also included a tab in the FEST analysis output file showing all clones that satisfied the above criteria with the exception of expansion compared with every other peptide. The user can then further analyze clones that expanded in response to more than one peptide, thus allowing for a breadth of bioinformatics on cross-reactive TCRs/peptides.

### MANAFEST can detect and track antitumor immune responses in patients receiving anti-PD-1

Although T-cell responses to viral antigens are often immunodominant (41–44), MANA-specific T cells are expected to be diverse and subdominant as well as functionally compromised (low cytokine production). We therefore considered that the breadth and magnitude of the endogenous immune response in cancer patients may be underestimated using ELISpot or multimer-based assays and that improved characterization of this response could be attained by using the FEST assay approach. Moreover, immune monitoring of the clinical response to checkpoint blockade requires T-cell clonotype tracking in tissue and longitudinal peripheral blood samples to confirm the amplification of MANA-specific TCR Vβ clonotypes upon treatment, a parameter that is not achievable by ELISpot. As a proof of principle, we performed MANAFEST on cells obtained at the time of surgical resection from JH124, a patient with stage IIB squamous NSCLC who achieved a complete pathologic response following two doses of neoadjuvant nivolumab (humanized antibody to PD-1; ref. 16). As previously reported, whole-exome sequencing was performed in pretreatment tumor and matched normal tissue and tumor-specific alterations were analyzed using a neoantigen prediction pipeline to identify candidate MANAs specific to the patient's HLA haplotype (16). T cells obtained 4 weeks after initiation of nivolumab were cultured for 10 days with 1 of 47 putative MANAs (Supplementary Table S7) and resulting expanded CD8$^{+}$ T cells were isolated for TCR Vβ CDR3 sequencing and MANAFEST analysis.

Following culture with predicted MANAs, 15 clonotypes were expanded relative to the "no peptide" control. The level of

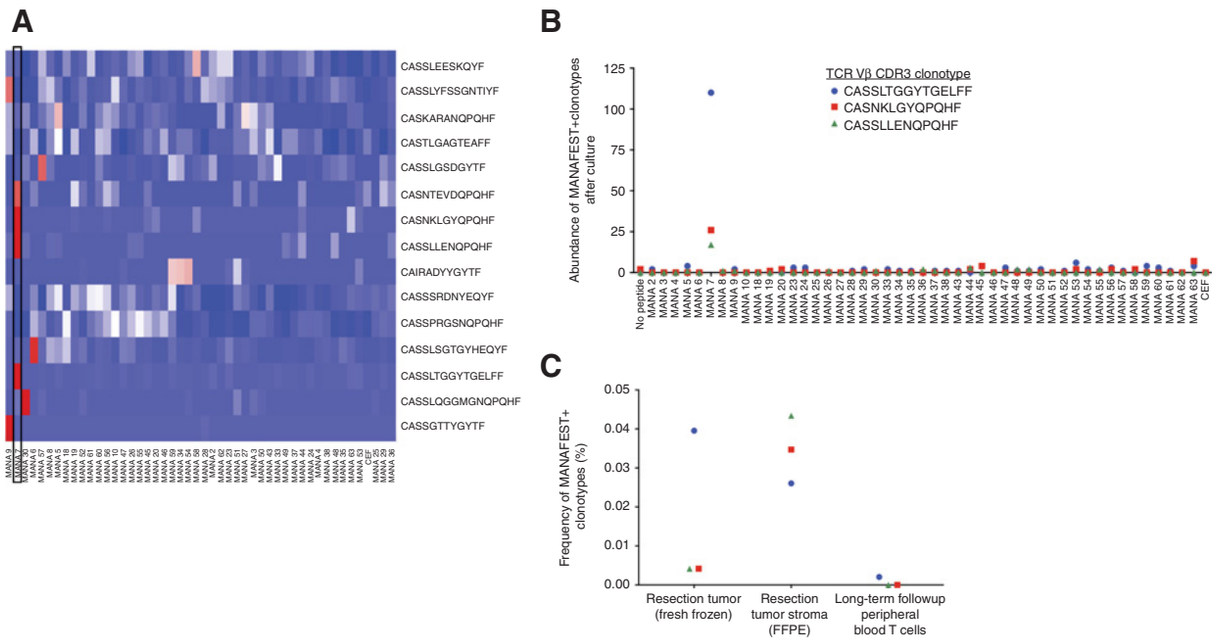


**Figure 5.**

The MANAFEST assay identifies multiple recognized MANAs and provides TCR barcodes to enable tracking of the antitumor immune response in tissue and peripheral blood. Recognition of candidate MANAs was evaluated by the MANAFEST assay in PBMCs obtained at the time of surgical resection from JH124, a patient with NSCLC being treated with neoadjuvant anti–PD-1. **A,** A heatmap generated by the FEST analysis platform shows all MANA/clone pairs to which significant antigen-specific expansion was detected, with expansions to MANA #7 outlined in black. **B,** T-cell clonotypes specific for MANA #7 as determined by the FEST analysis platform are shown as the number of sequencing templates (cells) detected after culture (abundance). **C,** The frequency (%) of each of these clonotypes among all templates detected via TCRseq is also shown in posttreatment fresh-frozen and FFPE tissue and in peripheral blood obtained >1 year after surgical resection. The parameters used for this analysis are shown in Supplementary Data S2. The FDR for the CASSLTGGYTGELFF clonotype was $5.63 \times 10^{-22}$ and the FDR for the CASNKLGYQPQHF and CASSLLENQPQHF clonotypes was 0.001. These 3 clonotypes were also identified as being specific for MANA #7 in an assay of T cells obtained from this patient 44 days after surgical resection (16).

specificity is illustrated by a heat map showing the fold change relative to control for each expanded clone (Fig. 5A). The MANAFEST analysis platform identified 4 of 47 putative MANAs that induced specific T-cell expansions (Supplementary Data S2). Of the 6 clonotypes that were expanded in response to these 4 MANAs, 3 clones specific for the putative HLA A*25:01-restricted EVIVPLSGW MANA, derived from a somatic sequence alteration in the *ARVCF* gene, were detected in the primary tumor (Fig. 5B; Supplementary Table S7). These 3 clonotypes were also detected in a previously reported assay of this patient's T cells, obtained 44 days after surgical resection, and underwent peripheral expansion upon nivolumab administration that decreased by 10 weeks after the first dose (16). The frequency of these clonotypes was also tracked in pre- and posttreatment FFPE tissue and posttreatment fresh-frozen tissue that underwent TCRseq. We additionally show here the representation of these clonotypes in fresh-frozen dissociated tumor tissue, FFPE tumor stroma, and peripheral blood obtained >1 year after surgical resection (Fig. 5C), thereby showing the utility of this assay in tracking antigen-specific TCR clonotypes in a multitude of biological compartments regardless of the availability of live cells. Aside from the abundance and frequency after culture, in tissue, and in serial peripheral blood samples, additional FEST output parameters can be correlated with treatment response (see output for patient JH124 in Supplementary Data S2). These parameters include the magnitude of *in vitro* expansion compared with uncultured T cells and to the "no peptide" control condition, the number of clones that are expanded in response to a given candidate MANA, and the sum frequency of FEST-positive clones in response to each peptide epitope after culture.

## Discussion

The development of personalized cancer immunotherapies as well as the need for biomarkers predictive of immunotherapy responses calls for routine high-throughput assays that monitor the antitumor immune response (1). These assays could measure the efficiency of the immunotherapeutic treatment and could also determine the eligibility of patients for immunotherapy, based on detection of a preexisting antitumor immune response (45). Improvements in DNA sequencing technologies have enabled characterization of mutations in the tumor exome and the TCR recognizing the neoantigens derived from these mutations (46, 47). Because amplification of selective TCRVβ clonotypes in tumor tissue has been proposed as a surrogate biomarker of MANA recognition (48), we introduce here the MANAFEST assay that is based on tumor exome-guided identification of predicted MANAs and the measure of the MANA-specific TCR clonotypic amplification following patient T-cell *in vitro* stimulation. We show that epitope-triggered clonal expansion can be observed in the absence of detectable IFNγ production, and that ELISpot likely underestimates the peripheral T-cell response. Furthermore, TCR sequencing underscores the diversity of the T-cell response

to a single HLA-restricted epitope. Altogether, our results validate TCR sequencing of a 10-day peptide-stimulated culture as the experimental core of the functional expansion of specific T cells (FEST) assays to monitor antigen-specific T-cell responses.

The FEST assays are sensitive and specific, and enable the tracking of antigen-specific TCR clonotype dynamics in T-cell DNA derived from tissues and peripheral blood. Combining peptide-stimulated cell culture and TCRseq with a bioinformatic platform, we provide the possibility to document the MANA specificity of TCR clonotypes and use these sequences as molecular tags to detect and quantify the antigen-specific T-cell response in all biological compartments (blood and tissues, fresh-frozen or fixed), a feature not achievable by other currently available cellular assays. This approach can therefore inform on the spatiotemporal dimension of the antimutanome TCR repertoire in serial blood samples, different distant cancer lesions (biopsies), and differential geographic regions in the same tumor (compatible with laser capture microdissection). FEST can be used to detect virus- and MANA-specific responses with greater sensitivity and throughput than current methods and can be expanded to a variety of antigens including tumor-associated antigens (TAAFEST), viral antigens (VIRAFEST), bacterial antigens (BactiFEST), and autoantigens (AutoFEST). This assay is an improvement over others limited by the low frequency and functional state of the T cells (ELISpot), HLA availability for multimer approaches (combinatorial encoding multimer), and the inadequacy of routine high-throughput clinical monitoring (ELISpot). The MANAFEST method has already been used to detect and monitor peripheral and intratumoral MANA-specific T-cell responses in NSCLC patients with acquired resistance to checkpoint blockade (17) and a colorectal cancer patient with a sustained partial response to pembrolizumab (29). Additionally, the robustness and reproducibility of this assay in detecting MANA-specific clonotypes is established by our detection of the same 3 clonotypes expanding in response to the same MANA in peripheral blood T cells obtained at the time of surgical resection, as described here, and 44 days after surgical resection, as described previously (16).

FEST-based monitoring provides metrics such as the intensity (magnitude of expansion), diversity (distinct unique CDR3 sequences), dynamics (unique sequence reads at different time points), and geographic distribution (tissue-resident and periphery) of the antitumor immune response. These metrics can be further interrogated in the context of homologous TCR motifs (49, 50). In comparison with existing methods, such as ELISpot and multimer approaches, we show that the setup of the test is feasible, using direct incubation of peptides with patient T cells, does not require specialized equipment such as a multiparameter flow cytometer or an ELISpot reader, permits higher throughput, and facilitates multicenter standardization for data sharing, databasing, and computational identification of biomarkers.

Because the test does not require the derivation of autologous antigen-presenting cells as required for the TMG approach, fewer numbers of PBMCs and therefore smaller samples are necessary to detect MANA-specific T cells. NGS has become relatively affordable and routine in patients receiving immunotherapy and clinical use of whole-exome sequencing may be envisaged in the future. In the context of widespread use of immunotherapy, the characteristics aforementioned may facilitate the compatibility with clinical practice (liquid biopsy) and improved patient comfort (noninvasive sampling). The computational pipeline to predict HLA-restricted MANAs and the web-based analysis used to identify immunogenic MANAs by FEST-based assays allow flexibility in decision making regarding the selection of MANAs to accommodate high or low mutational density and in the determination of a positive MANA-specific response by modifying the desired alpha and OR threshold. Although the assays described here evaluated MHC class I–restricted responses, we reason that this assay can be adapted to assess $CD4^+$/MHC class II–restricted responses as well. Additionally, because antigen-specific regulatory T cells are of particular interest in cancer patients, this T-cell subpopulation could be assayed using the FEST approach.

MANAFEST brings scientific and translational value, owing to the capacity for molecular characterization of the TCR sequences associated with MANA recognition that can be coordinated across patients or histologies and between institutions to identify common genomic features associated with immunogenicity of tumors and common structural motifs of the TCR (51). A central repository of these data would help define molecular motifs that could inform on the capacity of cancer patients to mount immune responses to their cancer and on their eligibility for immune checkpoint modulation. Upon clinical validation, the MANAFEST assay is therefore set to serve as a pan-cancer predictor of response to immunotherapy.

## Disclosure of Potential Conflicts of Interest

J. Naidoo reports receiving commercial research funding from Merck and AstraZeneca, and is a consultant/advisory board member for Bristol-Myers Squibb, AstraZeneca, and Takeda. J.R. Brahmer reports receiving commercial research funding from Bristol-Myers Squibb, Merck, and AstraZeneca, and is a consultant/advisory board member for Merck, Celgene, Eli Lilly, Bristol-Myers Squibb, Amgen, Genentech, and Syndax. P.M Forde reports receiving commercial research funding from Bristol-Myers Squibb, AstraZeneca, Novartis, and Kyowa, and is a consultant/advisory board member for Bristol-Myers Squibb, AstraZeneca, Novartis, Merck, Boehringer Ingelheim, and EMD Serono. V.E. Velculescu has ownership interest in and is a consultant/advisory board member for Personal Genome Diagnostics. D.M. Pardoll reports receiving commercial research funding from Bristol-Myers Squibb and has ownership interest in unlicensed patents covering material provided in the manuscript. K.N. Smith reports receiving commercial research funding from Bristol-Myers Squibb. No potential conflicts of interest were disclosed by the other authors.

## Authors' Contributions

**Conception and design:** V. Anagnostou, P.M. Forde, V.E. Velculescu, D.M. Pardoll, F. Housseau, K.N. Smith

**Development of methodology:** L. Danilova, V. Anagnostou, J.-W. Sidhom, A.S. Baras, L. Cope, V.E. Velculescu, F. Housseau, K.N. Smith

**Acquisition of data (provided animals, acquired and managed patients, provided facilities, etc.):** J.X. Caushi, H. Guo, H.Y. Chan, P. Suri, A. Tam, K.A. Marrone, J. Naidoo, J.R. Brahmer, P.M. Forde, F. Housseau, K.N. Smith

**Analysis and interpretation of data (e.g., statistical analysis, biostatistics, computational analysis):** L. Danilova, J.-W. Sidhom, J. Zhang, M. El Asmar, J. Naidoo, J.R. Brahmer, A.S. Baras, L. Cope, F. Housseau, K.N. Smith

**Writing, review, and/or revision of the manuscript:** L. Danilova, V. Anagnostou, J.X. Caushi, J.-W. Sidhom, H.Y. Chan, P. Suri, M. El Asmar, K.A. Marrone, J. Naidoo, J.R. Brahmer, P.M. Forde, L. Cope, V.E. Velculescu, D.M. Pardoll, F. Housseau, K.N. Smith

**Administrative, technical, or material support (i.e., reporting or organizing data, constructing databases):** J. Naidoo, A.S. Baras, F. Housseau, K.N. Smith

**Study supervision:** P.M. Forde, A.S. Baras, F. Housseau, K.N. Smith

## Acknowledgments

K.N. Smith and H.Y. Chan were funded by The Lung Cancer Foundation of America/International Association for the Study of Lung Cancer. F. Housseau

was funded by NIH R01 CA203891-01A1. K.N. Smith, H. Guo, P. Forde, and J.R. Brahmer were funded by a Stand Up To Cancer – Cancer Research Institute Cancer Immunology Dream Team Translational Research Grant (SU2C-AACR-DT1012). Stand Up To Cancer is a division of the Entertainment Industry Foundation. Research grants are administered by the American Association for Cancer Research, the Scientific Partner of SU2C. K.N. Smith, J.W. Sidhom, J. Zhang, A.S. Baras, and D.M. Pardoll were funded by the Mark Foundation for Cancer Research (grant MFCR-MIC-001). V. Anagnostou was funded by the Eastern Cooperative Oncology Group American College of Radiology Imaging Network and MacMillan Foundation. V.E. Velculescu was funded by U.S. National Institutes of Health grants CA121113, CA180950, the Dr. Miriam and Sheldon G. Adelson Medical Research Foundation, and the Commonwealth Foundation. All authors were funded by The Bloomberg-Kimmel Institute for Cancer Immunotherapy, Bloomberg Philanthropies, and NIH Cancer Center Support Grant P30 CA006973.

We would like to thank the healthy donors, patients, and their families for participation in this study, as well as the respective research and administrative teams that contributed to this study.

The costs of publication of this article were defrayed in part by the payment of page charges. This article must therefore be hereby marked *advertisement* in accordance with 18 U.S.C. Section 1734 solely to indicate this fact.

Received March 2, 2018; revised April 12, 2018; accepted June 4, 2018; published first June 12, 2018.

## References

1. Couzin-Frankel J. Breakthrough of the year 2013. Cancer Immunotherapy Science 2013;342:1432–3.
2. Lu YC, Robbins PF. Targeting neoantigens for cancer immunotherapy. Int Immunol 2016;28:365–70.
3. Yee C, Greenberg P. Modulating T-cell immunity to tumours: new strategies for monitoring T-cell responses. Nat Rev Cancer 2002;2:409–19.
4. Moodie Z, Price L, Gouttefangeas C, Mander A, Janetzki S, Lower M, et al. Response definition criteria for ELISPOT assays revisited. Cancer Immunol Immunother 2010;59:1489–501.
5. Craig FE, Foon KA. Flow cytometric immunophenotyping for hematologic neoplasms. Blood 2008;111:3941–67.
6. Meyer AL, Trollmo C, Crawford F, Marrack P, Steere AC, Huber BT, et al. Direct enumeration of Borrelia-reactive CD4 T cells ex vivo by using MHC class II tetramers. Proc Natl Acad Sci USA 2000;97:11433–8.
7. Barnes E, Ward SM, Kasprowicz VO, Dusheiko G, Klenerman P, Lucas M. Ultra-sensitive class I tetramer analysis reveals previously undetectable populations of antiviral CD8+ T cells. Eur J Immunol 2004;34:1570–7.
8. Tran E, Ahmadzadeh M, Lu YC, Gros A, Turcotte S, Robbins PF, et al. Immunogenicity of somatic mutations in human gastrointestinal cancers. Science 2015;350:1387–90.
9. Lu YC, Yao X, Crystal JS, Li YF, El-Gamil M, Gross C, et al. Efficient identification of mutated cancer antigens recognized by T cells associated with durable tumor regressions. Clin Cancer Res 2014;20:3401–10.
10. Andersen RS, Kvistborg P, Frosig TM, Pedersen NW, Lyngaa R, Bakker AH, et al. Parallel detection of antigen-specific T cell responses by combinatorial encoding of MHC multimers. Nat Protoc 2012;7:891–902.
11. Iezzi G, Karjalainen K, Lanzavecchia A. The duration of antigenic stimulation determines the fate of naive and effector T cells. Immunity 1998;8:89–95.
12. Wells AD, Gudmundsdottir H, Turka LA. Following the fate of individual T cells throughout activation and clonal expansion. Signals from T cell receptor and CD28 differentially regulate the induction and duration of a proliferative response. J Clin Invest 1997;100:3173–83.
13. Sun J, Dirden-Kramer B, Ito K, Ernst PB, Van Houten N. Antigen-specific T cell activation and proliferation during oral tolerance induction. J Immunol 1999;162:5868–75.
14. Carlson CS, Emerson RO, Sherwood AM, Desmarais C, Chung MW, Parsons JM, et al. Using synthetic templates to design an unbiased multiplex PCR assay. Nat Commun 2013;4:2680.
15. Robins HS, Campregher PV, Srivastava SK, Wacher A, Turtle CJ, Kahsai O, et al. Comprehensive assessment of T-cell receptor beta-chain diversity in alphabeta T cells. Blood 2009;114:4099–107.
16. Forde PM, Chaft JE, Smith KN, Anagnostou V, Cottrell TR, Hellmann MD, et al. Neoadjuvant PD-1 blockade in resectable lung cancer. N Engl J Med 2018;378:1976–86.
17. Anagnostou V, Smith KN, Forde PM, Niknafs N, Bhattacharya R, White J, et al. Evolution of neoantigen landscape during immune checkpoint blockade in non-small cell lung cancer. Cancer Discov 2017;7:264–76.
18. Jones S, Anagnostou V, Lytle K, Parpart-Li S, Nesselbush M, Riley DR, et al. Personalized genomic analyses for cancer mutation discovery and interpretation. Sci Transl Med 2015;7:283ra53.
19. Sausen M, Leary RJ, Jones S, Wu J, Reynolds CP, Liu X, et al. Integrated genomic analyses identify ARID1A and ARID1B alterations in the childhood cancer neuroblastoma. Nature genetics 2013;45:12–7.
20. Bertotti A, Papp E, Jones S, Adleff V, Anagnostou V, Lupo B, et al. The genomic landscape of response to EGFR blockade in colorectal cancer. Nature 2015;526:263–7.
21. Needleman SB, Wunsch CD. A general method applicable to the search for similarities in the amino acid sequence of two proteins. J Mol Biol 1970;48:443–53.
22. UCSC. https://genome.ucsc.edu/.
23. Szolek A, Schubert B, Mohr C, Sturm M, Feldhahn M, Kohlbacher O. OptiType: precision HLA typing from next-generation sequencing data. Bioinformatics 2014;30:3310–6.
24. Nielsen M, Andreatta M. NetMHCpan-3.0; improved prediction of binding to MHC class I molecules integrating information from multiple receptor and peptide length datasets. Genome Med 2016;8:33.
25. Lundegaard C, Lamberth K, Harndahl M, Buus S, Lund O, Nielsen M. NetMHC-3.0: accurate web accessible predictions of human, mouse and monkey MHC class I affinities for peptides of length 8–11. Nucleic Acids Res 2008;36:W509–12.
26. Lundegaard C, Lund O, Nielsen M. Accurate approximation method for prediction of class I MHC affinities for peptides of length 8, 10 and 11 using prediction tools trained on 9mers. Bioinformatics 2008;24:1397–8.
27. Stranzl T, Larsen MV, Lundegaard C, Nielsen M. NetCTLpan: pan-specific MHC class I pathway epitope predictions. Immunogenetics 2010;62:357–68.
28. Kim Y, Sidney J, Pinilla C, Sette A, Peters B. Derivation of an amino acid similarity matrix for peptide: MHC binding and its application as a Bayesian prior. BMC Bioinformatics 2009;10:394.
29. Le DT, Durham JN, Smith KN, Wang H, Bartlett BR, Aulakh LK, et al. Mismatch repair deficiency predicts response of solid tumors to PD-1 blockade. Science 2017;357:409–13.
30. Team RC. R: A language and environment for statistical computing. Vienna, Austria: R Foundation for Statistical Computing; 2014.
31. Gentleman RC, Carey VJ, Bates DM, Bolstad B, Dettling M, Dudoit S, et al. Bioconductor: open software development for computational biology and bioinformatics. Genome Biol 2004;5:R80.
32. Benjamini Y, Hochberg Y. Controlling the false discovery rate - a practical and powerful approach to multiple testing. J Roy Stat Soc B Met 1995;57:289–300.
33. Chang W, Cheng J, Allaire JJ, Xie Y, McPherson J. shiny: Web Application Framework for R. R package version 1.0.0 2017.
34. Price DA, Asher TE, Wilson NA, Nason MC, Brenchley JM, Metzler IS, et al. Public clonotype usage identifies protective Gag-specific CD8+ T cell responses in SIV infection. J Exp Med 2009;206:923–36.
35. Valkenburg SA, Josephs TM, Clemens EB, Grant EJ, Nguyen TH, Wang GC, et al. Molecular basis for universal HLA-A*0201-restricted CD8+ T-cell immunity against influenza viruses. Proc Natl Acad Sci USA 2016;113:4440–5.
36. Du VY, Bansal A, Carlson J, Salazar-Gonzalez JF, Salazar MG, Ladell K, et al. HIV-1-Specific CD8 T cells exhibit limited cross-reactivity during acute infection. J Immunol 2016;196:3276–86.
37. Kloverpris HN, McGregor R, McLaren JE, Ladell K, Harndahl M, Stryhn A, et al. CD8+ TCR bias and immunodominance in HIV-1 infection. J Immunol 2015;194:5329–45.
38. Hill BJ, Darrah PA, Ende Z, Ambrozak DR, Quinn KM, Darko S, et al. Epitope specificity delimits the functional capabilities of vaccine-induced CD8 T cell populations. J Immunol 2014;193:5626–36.

39. Sidney J, Southwood S, Mann DL, Fernandez-Vina MA, Newman MJ, Sette A. Majority of peptides binding HLA-A*0201 with high affinity crossreact with other A2-supertype molecules. Hum Immunol 2001; 62:1200–16.
40. Rammensee HG, Falk K, Rotzschke O. Peptides naturally presented by MHC class I molecules. Annu Rev Immunol 1993;11:213–44.
41. Motozono C, Kuse N, Sun X, Rizkallah PJ, Fuller A, Oka S, et al. Molecular basis of a dominant T cell response to an HIV reverse transcriptase 8-mer epitope presented by the protective allele HLA-B*51:01. J Immunol 2014;192:3428–34.
42. Wu C, Zanker D, Valkenburg S, Tan B, Kedzierska K, Zou QM, et al. Systematic identification of immunodominant CD8+ T-cell responses to influenza A virus in HLA-A2 individuals. Proc Natl Acad Sci USA 2011;108:9178–83.
43. Steven NM, Annels NE, Kumar A, Leese AM, Kurilla MG, Rickinson AB. Immediate early and early lytic cycle proteins are frequent targets of the Epstein-Barr virus-induced cytotoxic T cell response. J Exp Med 1997; 185:1605–17.
44. Betts MR, Nason MC, West SM, De Rosa SC, Migueles SA, Abraham J, et al. HIV nonprogressors preferentially maintain highly functional HIV-specific CD8+ T cells. Blood 2006;107:4781–9.
45. Topalian SL, Taube JM, Anders RA, Pardoll DM. Mechanism-driven biomarkers to guide immune checkpoint blockade in cancer therapy. Nat Rev Cancer 2016;16:275–87.
46. Kirsch I, Vignali M, Robins H. T-cell receptor profiling in cancer. Mol Oncol 2015;9:2063–70.
47. Vogelstein B, Papadopoulos N, Velculescu VE, Zhou S, Diaz LA Jr., Kinzler KW. Cancer genome landscapes. Science 2013;339:1546–58.
48. Pasetto A, Gros A, Robbins PF, Deniger DC, Prickett TD, Matus-Nicodemos R, et al. Tumor- and neoantigen-reactive T-cell receptors can be identified based on their frequency in fresh tumor. Cancer Immunol Res 2016;4: 734–43.
49. Sidhom JW, Bessell CA, Havel JJ, Kosmides A, Chan TA, Schneck JP. ImmunoMap: a bioinformatics tool for T-cell repertoire analysis. Cancer Immunol Res 2017;6:151–62.
50. Glanville J, Huang H, Nau A, Hatton O, Wagar LE, Rubelt F, et al. Identifying specificity groups in the T cell receptor repertoire. Nature 2017;547:94–8.
51. Faham M, Carlton V, Moorhead M, Zheng J, Klinger M, Pepin F, et al. Discovery of T-cell receptor beta motifs specific to HLA-B27(+) ankylosing spondylitis by deep repertoire sequence analysis. Arthritis Rheumatol 2017;69:774–84.